

Observation of Nucleation and Growth of CdS Nanocrystals in a Two-Phase System

Daocheng Pan,^{†,‡} Xiangling Ji,[‡] Lijia An,^{*,‡} and Yunfeng Lu^{*,†}

Department of Chemical Engineering, University of California, Los Angeles, California 90095, and State Key Laboratory of Polymer Physics and Chemistry, Changchun Institute of Applied Chemistry, Graduate School of the Chinese Academy of Sciences, Chinese Academy of Sciences, 5625 Renmin Street, Changchun 130022, China

Received August 21, 2007. Revised Manuscript Received February 4, 2008

The nucleation and growth kinetics of CdS nanocrystals in a two-phase synthesis system have been investigated. It was found that the nucleation process is quite lengthy and overlapped with the growth process; nevertheless, as formed nanocrystals show extremely narrow size distribution owing to the unique heterogeneous reacting environment and Ostwald ripening growth. The nucleation and growth kinetics of the nanocrystals were also influenced strongly by the monomer concentration, capping agent concentration, and solvent polarity. It was also found that a high monomer concentration, a low capping agent concentration, and low solvent polarity lead to a higher maximum nucleus concentration and nanocrystal concentration, while high polarity solvents are favorable for the formation of nanocrystals with narrower size distribution and higher photoluminescence quantum yield.

Introduction

Semiconductor quantum dots have attracted tremendous attention because of their unique optical and electronic properties that are highly size-dependent. Realizing the control over size and size distribution of quantum dots is therefore critical for both fundamental studies and real-world applications. To date, a large variety of semiconductor quantum dots have been synthesized either through a one-phase^{1–7} or a two-phase synthesis method.^{8–12} The former method involves the reacting molecular monomers at high temperature in a homogeneous solution,^{6,7} where a clear separation of nucleation and growth step is preferred

to ensure a narrow size distribution.^{1,3} The latter method involves reactions of molecular precursors in a heterogeneous solvent medium containing water and an organic solvent like toluene. Compared with the one-phase systems, the two-phase systems experience a much longer nucleation step overlapped with the growth step; nonetheless, as formed quantum dots (e.g., CdS,⁸ CdSe,⁹ TiO₂,¹⁰ ZrO₂,¹¹ and SnO₂¹²) do show extremely narrow size distribution. Elucidating the nucleation and growth process of quantum dots in the two-phase synthesis is therefore of great interest. Using the synthesis of CdS quantum dots as a model system, this work attempts to elucidate the nucleation and growth process in a two-phase system. The effects of monomer concentration, capping-agent concentration, and solvent polarity on the nucleation and growth kinetics were also systematically investigated using a simple ultraviolet–visible (UV–vis) spectroscopic technique.¹³

Experimental Section

Cadmium oxide (CdO, 99.5%), myristic acid (MA, 99.5%), oleic acid (OA, 90%), 1-octadecene (ODE, 90%), chlorobenzene (98%), toluene (99%), octane (98%), and thiourea (99%) were purchased from Aldrich. Cadmium myristate (Cd-MA) was synthesized by reacting CdO with myristic acid at 210 °C for 10 min and purified by recrystallization from toluene.

CdS quantum dots were synthesized according to the previous approach.⁸ In a typical synthesis, 0.2268 g (0.4 mmol) of Cd-MA, 1.0 mL of OA, and 9.0 mL of toluene were added to a three-neck

* Corresponding authors. E-mail: ljan@ciac.jl.cn (L.A.) and luucla@ucla.edu (Y.L.).

[†] University of California.

[‡] Chinese Academy of Sciences.

- (1) Sugimoto, T. *Adv. Colloid Interface Sci.* **1987**, *28*, 65.
- (2) Park, J. S.; Privman, V.; Matijevic, E. *J. Phys. Chem. B* **2001**, *105*, 11630.
- (3) Peng, X. G.; Wickham, J.; Alivisatos, A. P. *J. Am. Chem. Soc.* **1998**, *120*, 5343.
- (4) Talapin, D. V.; Rogach, A. L.; Haase, M.; Weller, H. *J. Phys. Chem. B* **2001**, *105*, 12278.
- (5) Rogach, A. L.; Talapin, D. V.; Shevchenko, E. V.; Kornowski, I. A.; Haase, M.; Weller, H. *Adv. Funct. Mater.* **2002**, *12*, 653.
- (6) Qu, L.; Yu, W. W.; Peng, X. G. *Nano Lett.* **2004**, *4*, 465.
- (7) Bullen, C. R.; Mulvaney, P. *Nano. Lett.* **2004**, *4*, 2303.
- (8) Pan, D. C.; Jiang, S. C.; An, L. J.; Jiang, B. Z. *Adv. Mater.* **2004**, *16*, 982.
- (9) Pan, D. C.; Wang, Q.; Jiang, S. C.; Ji, X. L.; An, L. J. *Adv. Mater.* **2005**, *17*, 176.
- (10) Pan, D. C.; Zhao, N. N.; Wang, Q.; Jiang, S. C.; Ji, X. L.; An, L. J. *Adv. Mater.* **2005**, *17*, 1991.
- (11) Zhao, N. N.; Pan, D. C.; Nie, W.; Ji, X. L. *J. Am. Chem. Soc.* **2006**, *128*, 10118.
- (12) Pan, D. C.; Zhao, N. N.; Ji, X. L. To be submitted.

- (13) Yu, W. W.; Qu, L. H.; Guo, W. Z.; Peng, X. G. *Chem. Mater.* **2003**, *15*, 2854.

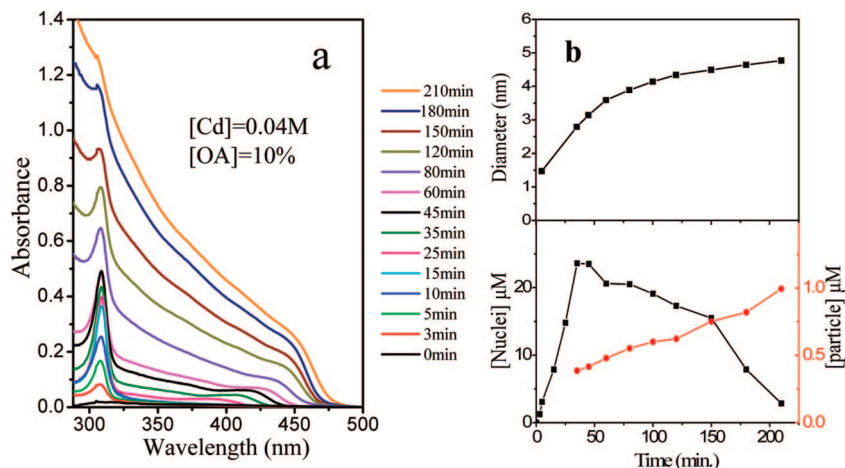


Figure 1. Left: temporal evolution of UV/vis absorption spectra of OA-capped CdS quantum dots synthesized with a cadmium precursor concentration of 0.04 M in toluene–water media. Right: Calculated size of the quantum dots (top) and concentration of the nuclei and quantum dots (bottom) as a function of time.

flask, and the mixture was heated to 95 °C for 10 min. A total of 78 mg (1.0 mmol) of thiourea was dissolved in 10 mL of water, and the solution was then injected into the flask under magnetic stirring. The reaction mixture was kept at 88 °C for 4 h. Aliquots of the solution (0.20 mL) were taken from the organic phase during the reaction when magnetic stirring was stopped and toluene and water were separated. As-taken solutions were precipitated with ethanol (~4 mL) and isolated by centrifugation and decantation. The purified quantum dots were then dispersed in 2.0 mL of toluene for UV–vis measurements.

UV–vis absorption spectra were recorded on a Shimadzu UV-1700 spectrometer using 1.0 cm quartz cell with a resolution of 0.5 nm. In this work, all measurements were performed ex-situ for two reasons. First, the reactions were conducted in a heterogeneous medium, which creates difficulty in performing in situ observation as compared with a single-phase system.^{6,14} Second, the nuclei exhibit an absorption maximum at 311 nm, while oleic acid and the unconverted cadmium precursor in a crude solution also show significant adsorption in the 300–400 nm region. Therefore, to actually measure the nuclei concentration, as obtained crude solution must be purified prior to the UV/vis measurement.

The size and molar concentration of the quantum dots were calculated according to the literature.¹³ Briefly, the size was calculated using the formula¹³ $D = (-6.6521 \times 10^{-8})\lambda^3 + (1.9557 \times 10^{-4})\lambda^2 - (9.2352 \times 10^{-2})\lambda + 13.29$, where D is the quantum-dot diameter and λ is the wavelength of first excitonic absorption peak. The molar extinction coefficient ϵ was calculated using the formula $\epsilon = 5500\Delta E D^{2.5}$, where ΔE is the transition energy (unit of eV) corresponding to the first absorption peak position. The molar concentration (C) was calculated using the Lambert–Beer's law, $A = \epsilon CL$, where A is absorbance intensity and L is optical path length (cm). Our experiment indicated that the molar extinction coefficient of CdS critical nuclei is independent of solvent polarity (e.g., octane and toluene; see Supporting Information, Figure S1).

Dynamic laser light scattering (DLS, Brookhaven 90 Plus) was used to determine the size of the nuclei. The measurements were performed at a fixed scattering angle of 90°. The low-angle X-ray diffraction patterns were recorded on a Siemens D-500 X-ray diffractometer in the range of 1–10°. Photoluminescence (PL) spectra were recorded on a Shimadzu RF-5301 PC fluorometer with

a resolution of 1.0 nm. Room temperature PL quantum yields (PL QYs) were calculated against coumarin 6 in ethanol as a standard sample (QY = 0.78). Transmission electron microscopy (TEM) images were taken on a JEOL-1011 electron microscope with an accelerating voltage of 100 kV. The size distribution of the nanocrystals was calculated from measuring the size of 200 particles in TEM images.

Results and Discussion

Generally, in a two-phase system, molecular precursors (e.g., Cd-MA and thiourea) are preferably separated within the organic (e.g., toluene) and the aqueous phase. Reactions of the precursors along the liquid–liquid interface generate nuclei that are stabilized by the capping agent (e.g., oleic acid). The oleic acid capped nuclei are hydrophobic and are dispersed preferably within the organic phase, which may either grow into quantum dots or be consumed through a ripening process during the reaction.

Figure 1a shows UV/vis absorption spectra of the critical nuclei and quantum dots at different reaction times using toluene/water as a reacting medium and a cadmium precursor concentration of 0.04 M. The absorption peaks at 311 nm are attributed to the critical nuclei.⁸ As shown in Figure 1a, the absorption intensity of critical nuclei gradually increases with time, reaches the maximum intensity at 15 min, and disappears after 210 min. Note that the intensifying adsorption at the longer wavelength during the nucleating process, which is attributed from the formation of quantum dots, was also observed. More interestingly, the band-edge absorption of the quantum dots red shifts toward the longer-wavelength direction, suggesting the growing nanocrystal size. To further quantify this dynamic process, size and concentration of the quantum dots, as well as concentration of the nuclei, were calculated and plotted in Figure 1b. Such a spectroscopic observation clearly suggests a dynamic formation process involving generation, consumption, and growth of the nuclei into quantum dots, which consists of (1) nucleation, (2) overlapped nucleation and growth, and (3) dominated growth stage.

Stage 1 is a dominated nucleation process characterized by the rapidly increased nuclei population and the absence

(14) Reiss, P.; Carayon, S.; Bleuse, J.; Pron, A. *Synth. Met.* **2003**, *139*, 649.

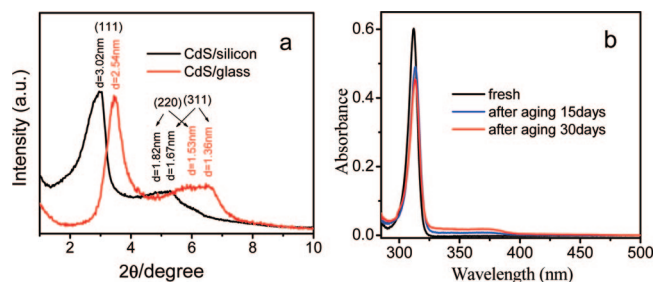


Figure 2. (a) Low-angle X-ray diffraction pattern of a nucleus superstructure assembled on hydrophobic silicon substrate and a hydrophilic glass substrate. (b) The UV-vis absorption spectra of the purified nuclei solution aged for 15 and 30 days.

of nanocrystal formation. Consistently, Figure 1a shows the intensifying nucleus adsorption at 311 nm with the absence of quantum-dot adsorption at the longer wavelength from 0 to 10 min. The nuclei isolated and purified during this stage are composed of Cd and S with an atomic ratio of 2:1 rather than 1:1 according to the energy dispersive X-ray analysis (EDX) (see Supporting Information Figure S2), because the outermost layer of the nuclei is composed mainly by cadmium atoms.^{15–20} Furthermore, the nuclei are monodisperse in size allowing their self-organization into a highly ordered superstructure. For example, Figure 2a shows the X-ray diffraction (XRD) pattern of a superstructure assembled by the OA-capped CdS nuclei on a hydrophilic glass substrate. This well defined diffraction pattern is consistent with a face-centered-cubic structure (fcc) with a unit cell parameter of 4.4 nm. Assembling the nuclei on a hydrophobic surface (e.g., HF-etched silicon surface) resulted in a superstructure with a larger unit cell parameter (5.2 nm), possibly due to more favorable hydrophobic interactions between the hydrophobic nuclei and the substrate surface. Recently, Kasuya et al.²¹ reported the formation of a similar fcc superstructure with a larger unit cell parameter of 5.5 nm from dodecylamine-capped CdSe nanoparticles with 1.5 nm diameter. Since oleic acid is longer than dodecylamine, these OA-capped CdS nuclei should have a diameter smaller than 1.5 nm, which is consistent with the dynamic light scattering (DLS) measurement (1.32 nm), as well as that calculated from the absorption spectrum (1.47 nm). Interestingly, we observed that the nucleus size is independent of the monomer concentration, capping agent concentration, solvent, or even reaction temperature,²² which was different to those reported previously.^{6,7}

Stage 2 is an overlapped nucleation-growth process characterized by the continuously increased nuclei population, as well as the increased nanocrystal population and size. During this stage (from 10 to 15 min), reactions of the precursors along the organic/water interface continuously generate nuclei and intensify the UV-vis absorption at 311 nm. Simultaneously, the absorption corresponding to the quantum dots appears and gradually intensifies as a result of nanocrystal formation and growth. The growth process may be achieved either by reacting the molecular precursors on the nucleus surface or by the Ostwald ripening of the nuclei, which can be monitored readily using the UV-vis spectroscopic technique. For example, Figure 2b shows the UV-vis spectra of a purified nuclei solution in toluene aged for different times at room temperature. The fresh nuclei solution only shows the characteristic nucleus absorption at 311 nm. After 15 days, a decreased absorption intensity at 311 nm and a new absorption band in the 320–390 nm region was observed, indicating the formation of larger-size nanocrystals through the Ostwald ripening process. Although it is difficult to exclude the aggregation growth mechanism, we believe that Ostwald ripening at least is the dominant mechanism due to the similar size for the nuclei (1.5 nm) and nanocrystals (4–5 nm). Consistently, absorption intensity of the nuclei further decreases accompanied by the further intensified nanocrystal absorption after 30 days. Such competition between the nucleus production and consumption results in the dynamic evolution of nucleus and nanocrystal concentration. Consequently, as shown in Figure 1a, the nucleus concentration continuously increases and reaches its maximum at 15 min, indicating a dominated nucleation process that is overlapped with a growth process.

Stage 3, the dominated growth period, begins when the nucleus concentration decreases from its maximum concentration. During this stage, consumption of the nuclei overwhelms their production, resulting in the decreasing nucleus population, increasing nanocrystal size, and increasing nanocrystal population as indicated by Figure 1b.

As discussed above, the nucleation and growth of nanocrystals in a two-phase system are quite lengthy and overlapped with the growth process; nevertheless, as formed nanocrystals are extremely narrowly distributed in size, possibly due to its unique two-phase reacting environment and nature of the Ostwald ripening process. More specifically, since the precursors are spatially separated in the organic and aqueous phase, except the growth of nanocrystals through Ostwald process in the organic phase, both nucleation and growth occur only at the organic–water interface. This requires nuclei or nanocrystals to diffuse to the organic–water interface prior to the further reactions. Although the nanocrystals and nuclei are capped with identical capping agent, their diffusion resistance is size-dependent. As a result, small nanocrystals grow faster and catch up with the large ones as long as the growth time is long enough, attributing to the formation of monodisperse nanocrystals.

- (15) Herron, N.; Calabrese, J. C.; Farneth, W. E.; Wang, Y. *Science* **1993**, *259*, 1462.
- (16) Vossmeier, T.; Reck, G.; Katsikas, L.; Haupt, E. T. K.; Schulz, B.; Weller, H. *Science* **1995**, *267*, 1476.
- (17) Lee, G. S. H.; Fisher, K. J.; Craig, D. C.; Scudder, M. L.; Dance, I. G. *J. Am. Chem. Soc.* **1990**, *112*, 6435.
- (18) Behrens, S.; Bettenhausen, M.; Eichhofer, A.; Fenske, D. *Angew. Chem., Int. Ed.* **1997**, *36*, 2797.
- (19) Soloviev, V. N.; Eichhofer, A.; Fenske, D.; Banin, U. *J. Am. Chem. Soc.* **2000**, *122*, 2673.
- (20) Gaumet, J. J.; Khitrov, G. A.; Strouse, J. F. *Nano Lett.* **2002**, *2*, 375.
- (21) Kasuya, A.; Sivamohan, R.; Barnakov, Y. A.; Dmitruk, I. M.; Nirasawa, T.; Romanyuk, V. R.; Kumar, V.; Mamykin, S. V.; Tohji, K.; Jeyadevan, B.; Shinoda, K.; Kudo, T.; Terasaki, O.; Liu, Z.; Belosludov, R. V.; Sundararajan, V.; Kawazoe, Y. *Nat. Mater.* **2004**, *3*, 99.
- (22) Wang, Q.; Pan, D. C.; Jiang, S. C.; Ji, X. L.; An, L. J.; Jiang, B. Z. *Chem. Eur. J.* **2005**, *11*, 3843.

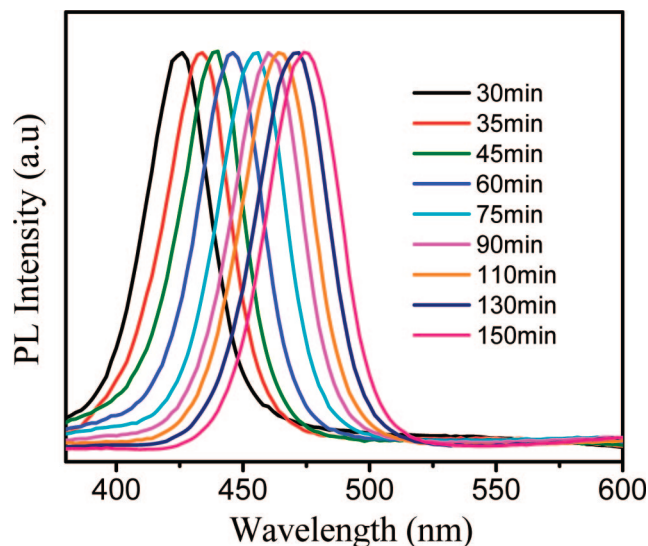


Figure 3. Temporal evolution of photoluminescence spectra of the OA-capped CdS nanocrystals during a reaction.

Another important reason may come from the nature of Ostwald ripening. As known, the Ostwald ripening process is driven by energy minimization, which allows growth of larger nanocrystals through consuming small ones. In fact, compared the maximum critical nuclei concentration and the final nanocrystal concentration, only few nuclei ($\sim 1\text{--}5\%$) are grown into the final nanocrystals, and the majority of the nuclei are consumed. A slow ripening process due to the low reaction temperature and slow reaction may also favor the formation of such monodisperse nanocrystals. Figure 3 shows PL spectra of OA-capped CdS nanocrystals at different reaction times. The fwhm (full width at half-maximum) in the photoluminescence spectra are maintained at about 25 nm when the reaction time is from 30 to 150 min, indicating that a narrower size distribution is maintained throughout the reaction. Such a time-independent size distribution is quite unique since most syntheses of nanocrystals from organometallic approach and its variants often exhibit time-dependent size distribution.^{3,6,23}

Compared with two-phase synthesis, the reactions in a homogeneous one-phase system^{6,7} occur much faster, resulting in much faster nucleation and growth that are generally difficult to monitor. Ostwald ripening occurs mainly after the depletion of precursor and subsequent quantum dot formation. To further understand the two-phase system, we examined the effects of monomer concentration, capping agent concentration, and polarity of the organic phase on the nucleation and growth.

1. Effect of Monomer Concentration. Figure 4 compares the time evolution of the nanocrystal size (top), nuclei concentration (middle), and quantum dot concentration (bottom) with initial cadmium precursor concentrations of 0.04 and 0.02 M, respectively. Lower nuclei and quantum dot concentrations, as well as smaller quantum dot size, are observed for the lower cadmium precursor concentration. The

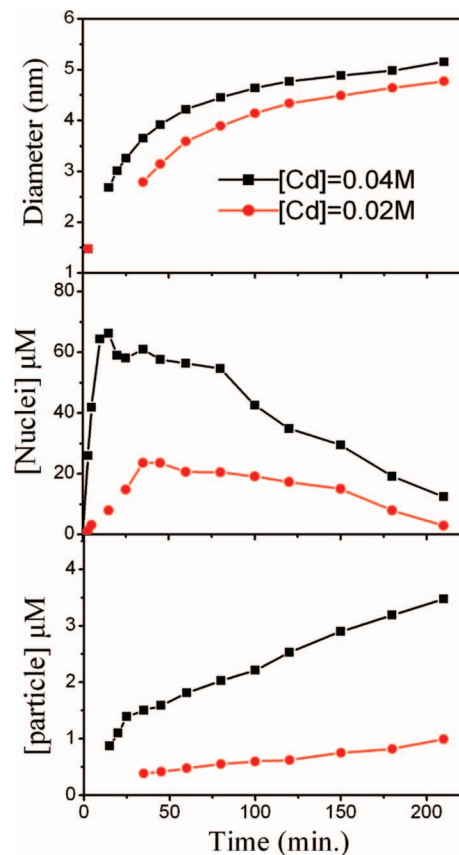


Figure 4. Comparison of the quantum dot size (top), critical nuclei concentration (middle), and quantum dot concentration (bottom) as a function of time with a cadmium precursor concentration of 0.04 and 0.02 M.

use of 0.04 M precursor led to a maximum concentration of nuclei of $66\ \mu\text{M}$, while decreasing the precursor concentration to 0.02 M resulted in a low concentration of $24\ \mu\text{M}$. This observation provides a simple and efficient route to tune the quantum dot diameter.

2. Effect of the Capping Agent. Capping agents may form stable complexes with molecular precursors or binding on the nanocrystal surface, which will slow down the nucleation and growth process. Figure 5a,b shows the temporal evolution of UV/vis absorption spectra of the quantum dots prepared with 10% and 5% (vol % in organic phase) concentrations of oleic acid, respectively. Much weaker absorption at the long wavelength region is observed at the high oleic acid concentration, indicating a slower nanocrystal formation process. The calculated nanocrystal size, nanocrystals, and nuclei concentration are also shown in Figure 5c. It clearly shows that increasing the concentration of oleic acid from 5% to 10% results in a decreased maximum nuclei concentration from 2.0 to 0.46 mM. As a result, a larger fraction of the cadmium precursor was retained for subsequent crystal growth, leading to the formation of larger nanocrystals after 4 h of reaction (Figure 5c). A longer reaction time allows a more mature nanocrystal growth through Ostwald ripening, which may further change the nanocrystal size and concentration. Moreover, an extremely high capping agent concentration may create a highly packed ligand layer on the nanocrystal surface, hindering monomer diffusion to the nanocrystal surface and their subsequent reactions. In fact, when 50% concentration of oleic acid was used, only a few nuclei

(23) Dai, Q.; Li, D.; Chen, H.; Kan, S.; Li, H.; Gao, S.; Hou, Y.; Liu, B.; Zou, G. *J. Phys. Chem. B* **2006**, *110*, 16508.

(24) Pan, D. C.; Wang, Q.; Ji, X. L.; An, L. J. *J. Phys. Chem. C* **2007**, *111*, 5661.

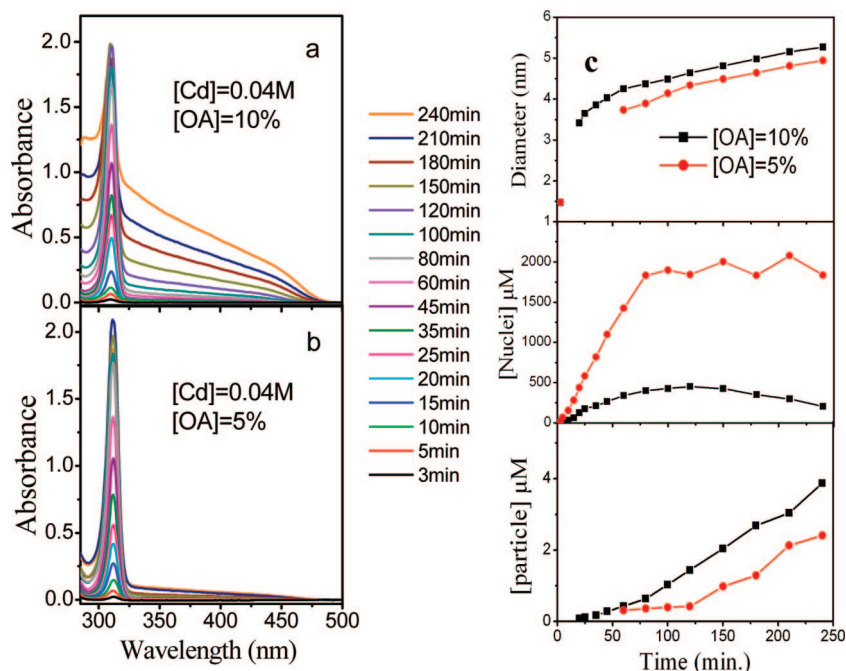


Figure 5. Left: temporal evolution of UV/vis absorption spectra of nanocrystals synthesized at different oleic acid concentrations in octane. Right: the calculated nanocrystal size (top), critical nuclei concentration (middle), and nanoparticle concentration (bottom).

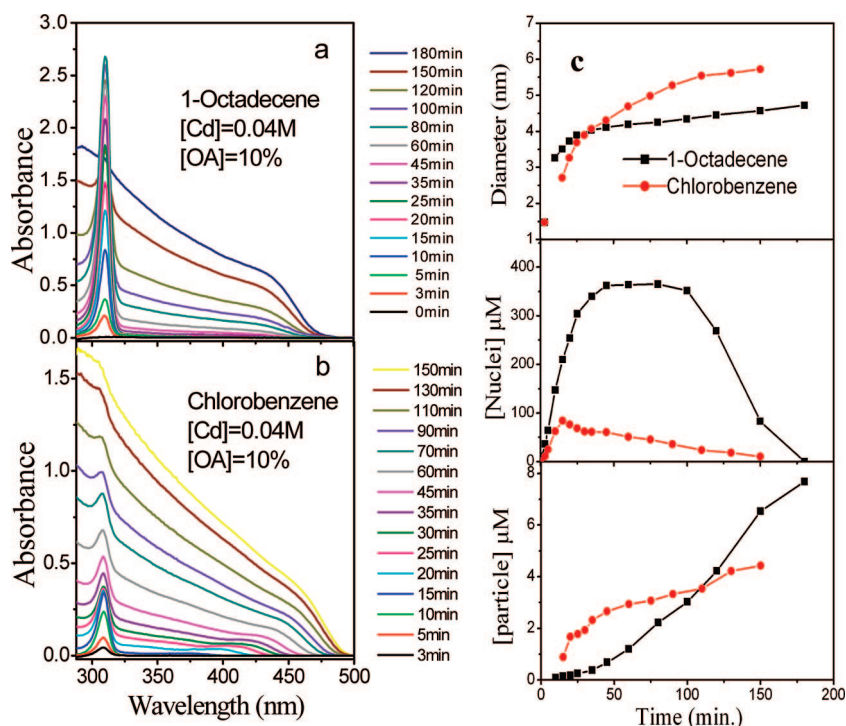


Figure 6. Left: UV/vis absorption spectra of nanocrystals synthesized in chlorobenzene and octadecene at different reaction times using $[Cd]_0 = 0.04$ M and $[OA]_0 = 10\%$ (vol % in organic phase). Right: the calculated nanocrystal size (top), nuclei concentration (middle), and nanocrystal concentration (bottom).

were observed in the UV/vis absorption spectrum even after 4 h of reaction.

Binding strength of ligands also strongly affects the nucleation and growth kinetics. For example, using *n*-trioctylphosphine oxide (TOPO), a weaker capping agent than OA resulted in a much faster nucleation and growth. On the contrary, the use of long-chain aliphatic thiols (e.g., dodecanethiol) will impede completely the nucleation and

growth because of much stronger complexation. The reaction does not occur even though the high reactivity Na_2S is used as a sulfur source.²⁴

3. Effects of Solvent Polarity. Figure 6a,b shows a series of UV/vis absorption spectra of OA-capped CdS nanocrystals synthesized in low polarity solvent (ODE) and high polarity solvent (chlorobenzene), respectively. Figure 6c shows the calculated particle size, critical nuclei concentration, and particle

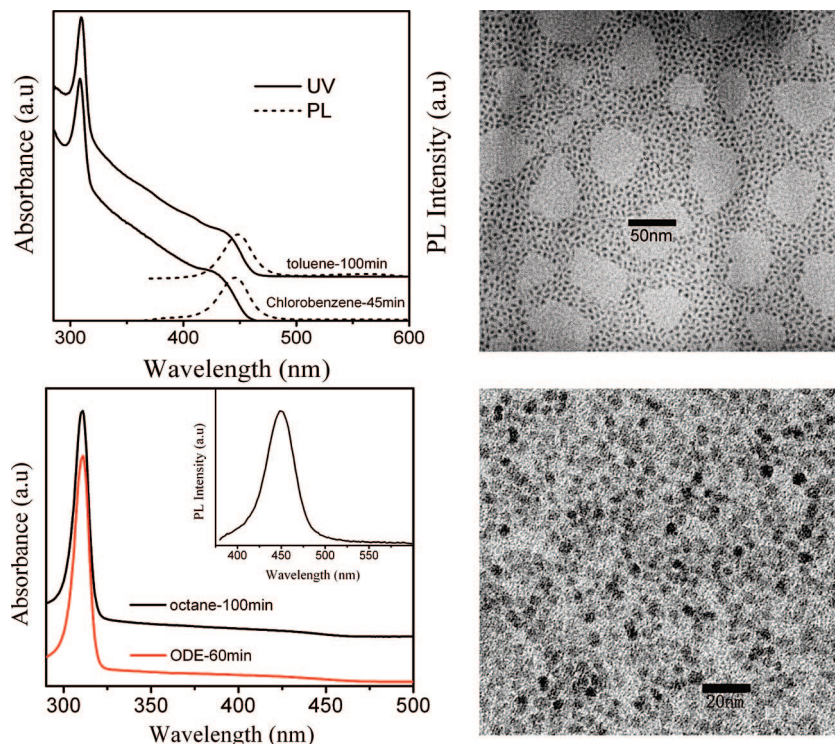


Figure 7. Left: UV/vis absorption and PL spectra of the nanocrystals with similar sizes synthesized in toluene and chlorobenzene (left top) and octane and ODE (left bottom). Inset: PL spectrum of the nanocrystals synthesized in ODE. Right: TEM images of the nanocrystals synthesized in toluene (right top) and ODE (right bottom).

concentration as a function of reaction time. As known, the OA-capped nuclei are hydrophobic and can be more easily dispersed in low polarity solvent. Consistently, we found that the maximum nucleus concentration in low polarity solvent is much higher than those in high polarity solvent (e.g., 400–500 μM vs 70–90 μM). Since a larger fraction of precursors was consumed to form the nuclei in the low polarity system, a higher concentration but smaller nanocrystals will be achieved (Figure 6c).

Solvent polarity also affects the size distribution and PL quantum yield of the nanocrystals. Figure 7 (left) shows the UV/vis absorption and PL spectra of the nanocrystals with a similar diameter (~ 4.8 nm) synthesized in four different solvents. The nanocrystals synthesized in high polarity solvent (toluene and chlorobenzene) show more evident first excitonic absorption peaks and narrower PL bands than those synthesized in low polarity solvent (octane and ODE). Figure 7 (right) shows TEM images of the nanocrystals synthesized in toluene (right top) and ODE (right bottom). The size distributions of nanocrystals synthesized in toluene and chlorobenzene are approximately 5–15% compared with 15–25% for those synthesized in lower polarity ODE and octane. The PL quantum yields for the nanocrystals synthesized in high polarity toluene or chlorobenzene are as high as 10–20% compared with 1–2% for those synthesized in low polarity octane or ODE. Therefore, a higher solvent polarity favors that formation of nanocrystals with narrower size distribution and higher quantum yield.

Recently, Talapin et al.⁴ studied the evolution of a nanosized particle in colloidal solution and proposed two general strategies to improve nanoparticle size distribution: (1) carrying out

nanoparticle growth process in a diffusion controlled regime or (2) increasing surface tension at the solvent–nanoparticle interface, for example, by choice of proper surfactants. Herein, we can also change the surface tension at the solvent–nanoparticle interface by changing the solvent polarity instead of changing surfactants. Since the OA-capped CdS nanocrystals are highly hydrophobic, surface tension at the solvent–nanoparticle interface should be larger in a higher polarity organic solvent. Such a high surface tension therefore favors the formation of nanocrystals with narrower size distribution and a higher PL QY. However, a high polarity may also have poor solubility for nanocrystals, which results in failure of the nanoparticle synthesis. For example, as formed nanocrystals may not be soluble in 1-heptanol.

Conclusions

The two-phase synthesis method is a highly efficient approach toward the synthesis of quantum dots with well-controlled particle size and size distribution. Although the nucleation and growth process of CdS nanocrystals is lengthy and even overlapped, as formed nanoparticles possess extremely narrow size distributions owing to the unique heterogeneous reacting environment and the unique Ostwald ripening growth. The nucleation and growth are influenced strongly by the monomer concentration, capping agent concentration, and noncoordinating solvent polarity. A higher monomer concentration, a lower capping agent concentration, and a lower solvent polarity lead to a higher maximum nucleus concentration and quantum dot concentration. It was also found that noncoordinating high polarity solvents are favorable for the formation of nanocrystals with narrower size distribution and higher photoluminescence quantum yield.

Acknowledgment. This work was supported by the Office of Naval Research (ONR), National Science Foundation (CA-REER), National Natural Science Foundation of China for General (50303017, 50373044, 50253002, 90101001) and Major (50290090, 20394006), the Special Pro-Funds for Major State Basic Research Projects (2002CCAD4000), the Special Funds for Major State Basic Research Projects (No. 2003CB615600) and the Distinguished Young Fund of Jilin Province (20050104), the Project (KJCX2-SW-H07) from the Chinese Academy of Sciences, and the International Collaboration Project (04-03GH268, 20050702-2) from Changchun City and Jilin Prov-

ince, China. The authors also thank Dr. Jiebin Pang in University of New Mexico for his helpful suggestions.

Supporting Information Available: UV/vis absorption spectra of the same CdS critical nuclei sample dissolved in toluene and octane and EDX spectrum of CdS critical nuclei (PDF). This material is available free of charge via the Internet at <http://pubs.acs.org>.

CM7023718